JOURNAL of
MATERIALS and MECHATRONICS:A

e-ISSN 2717-8811
JournalMM, 2024, 5(1), 36-48
https://doi.org/10.55546/jmm.1445220

Araştırma Makalesi / Research Article

Investigation of Three Body Abrasive Wear Behavior of Micro-Nano Sized Iron Ore Pieces on Bronze

Abdullah UĞUR[1*], Ahmet Emrah ERDOĞDU[2], Recep DEMİRSÖZ[3]

[1*]Karabük University, Faculty of Engineering, Department of Mechanical Engineering, Karabük, Turkey,
ORCID ID: https://orcid.org/0000-0002-3495-529X, augur@karabuk.edu.tr
[2] Karabük University, Faculty of Engineering, Department of Mechanical Engineering, Karabük, Turkey,
ORCID ID: https://orcid.org/ 0000-0003-1831-3972, aemraherdogdu@karabuk.edu.tr
[3] Karabük University, Faculty of Engineering, Department of Mechanical Engineering, Karabük, Turkey,
ORCID ID: https://orcid.org/ 0000-0003-0674-4572 , recepdemirsoz@karabuk.edu.tr

Geliş/ Received: 01.03.2024**;** **Revize/Revised:** 12.04.2024 **Kabul / Accepted:** 16.04.2024

ABSTRACT: In In this work, the three-body abrasive wear of bronze (C86200) in pig cart transmissions was examined. Micro-nano-sized ore particles were introduced to the lubricating media during the Ball-on-flat test to represent three-body abrasive wear. Load shear rate and lubricating medium were useful research inputs. Outputs included examining sample surfaces, mass loss, friction coefficient, and trace depth. Taguchi, ANOVA, and RSM were used to analyze experimental data. The most effective parameter for all outputs was the load value, with a rate of 55.76 percent, while the speed had the lowest influence on mass loss, at 9.74 percent. The regression model fits these results well.

Keywords: Three-Body Abrasive Wear, Ore Particle, Lubricated Environment, Bronze.

1. INTRODUCTION

Wear is a very common fundamental problem, especially in systems with movement and contact (Bozkurt et al., 2021; Huang et al., 2019; Sardar et al., 2018). To solve and understand this problem, which is encountered in a wide variety of fields, many different solution methods and situation analyzes are carried out by considering the effects of the problem (cost, time, comfort, safety, etc.) (Kusumoto et al., 2019). Wear mechanisms are affected and diversified by many similar variables, especially mechanical properties (force, speed, etc.), material-related factors (hardness, surface roughness, etc.) and environmental factors (PH, lubrication, chemical concentrations, etc.)(Akram et al., 2021; Cetin and Korkmaz, 2020; Radhika and Sai Charan, 2017) . One of the wear types is abrasive wear. In the case of abrasive wear, the wear mechanism can be two-body (Singh et al., 2022) or three-body (Varol et al., 2018). During three-body abrasive wear, there are also abrasive

*Sorumlu yazar / Corresponding author: augur@karabuk.edu.tr
Bu makaleye atıf yapmak için /To cite this article

Uğur, A., Erdoğdu, A. E, Demirsöz, R. (2024). Investigation of Three Body Abrasive Wear Behavior of Micro-Nano Sized Iron Ore Pieces on Bronze. Journal of Materials and Mechatronics: A (JournalMM), 5(1), 36-48.

particles, which can be considered as a third body, between two surfaces moving relative to each other (R.A. García-León et al., 2021; Liu et al., 2018). During three-body abrasive wear, the type, properties (size, hardness, etc.) and mechanical behavior of the abrasive particles are additional factors affecting wear (Gheisari and Polycarpou, 2018; Lan et al., 2017; Lan and Polycarpou, 2018). Although the three-body abrasive wear phenomenon is complex, it offers a more realistic wear approach, especially for dust and particulate media applications. Charging facilities, which are a part of the blast furnace process, can be given as an example to the raw material loading areas of the production facilities. The elements of the mechanical structures in these facilities that come into contact with each other are exposed to three-body abrasive wear from time to time due to the particles coming from the external environment (Manoharan et al., 2019). In addition, two-body wear mechanisms can also turn into three-body wear mechanisms. This event occurs when particles break off from one or both elements that make up the structure (Radhika, 2017). Today, it is seen that there are not enough studies on the three-body wear mechanism of bronze materials and the abrasive effect of ore particles as the third body (R. A. García-León et al., 2021a).

Purba et al. In their study, they examined the yield strength and tribological properties of the material they developed. For this, they carried out rubber wheel abrasive machine tests in different particle sizes in accordance with the ASTM G65 standard. As a result, they stated that the microstructure and abrasive size should be known in order to know the wear properties of alloys (Purba et al., 2023).

Xin et al. evaluated friction and wear of amorphous-nanocrystalline plasma-sprayed coatings with oil lubrication. The coating holds up effectively under modest strains and resists abrasive particles even at higher loads (Xin et al., 2022). Zhao et al. employed molecular dynamics simulations to study heterostructure films' tribological characteristics. This study found that self-rotating abrasives reduced friction and wear. This work revealed the molecular tribological characteristics of graphene/h-BN sheets (Zhao et al., 2022).

Studies on the three-body wear mechanisms of bronze materials and the abrasive effect of ore particles acting as the third body, particularly in micro-nano sized particles, are currently lacking. (Bharatish et al., 2018; Yin et al., 2020) . To fill this gap in the literature, this paper aims to contribute with the better understanding of the three-body abrasive behavior on bronze C86200 alloy materials. This study is about the effects of load and sliding speed on mass loss (ML), friction coefficient (CoF) and trace depth (TD) in different oil environments containing micro and nano (min.50 nm – max.2 μm) ore particles.

2. MATERIALS AND METHODS

Wear tests were carried out in Karabük University Engineering Faculty laboratories. The bronze material using as the test specimen was carried out with the help of a ball-on-flat type original test installation, in an environment containing only lubricant and in a lubricant environment in which micro-nano ore particle was added at two different rates. Experimental design and parameters are given in Table 1.

Table 1. Parameters and experimental design.

Factor levels	Factors			Distance (m)	Stroke length (mm)
	Load (N)	Ore Particle mass ration (%)	Sliding speed (mm/s)		
1	20	-	17.3	100	14
2	40	0.3	30.3		
3	60	0.6	43.3		

2.1 Material

In the study, special casting C86200 bronze material used in raw material manipulation systems was selected. The chemical composition of the bronze material is given in Table 2. The hardness, yield strength and surface roughness values of the C86200 material used are given in Table 3.

Table 2. Chemical composition of the brass specimen

Cu	Zn	Ni	Fe	Al	Si	S	Mn	Sn	Others
70.28	21.78	3.65	0.68	1.9	0.11	0.07	0.48	0.6	0.45

Table 3. Average hardness, yield strength and surface roughness values of the specimen

Average Hardness [HV]	Yield Stress [MPa]	Ra [μm]
212,3 (±4.92)	621	0.086-0.096

2.2 Abrasive Particles & Lubricant

The abrasive particles to be used in the three-body abrasion test were first taken from the ore heap to remain under the 25 μm sieve. Then, abrasive particle size was reduced by using the Fristch Pulverisette 7 Classic Line micro mill device. The milling process was obtained for each 14 g of abrasive ore particle, after a net 20-hour milling at 700 rpm for 5 minutes and 2 minutes of pause (Bailon-Poujol et al., 2011; Lakshmikanthan et al., 2019; Madhusudan et al., 2020). After the milling process, size measurements were made with the SEM device. The images and particle size measurements taken from the SEM device are given in Figure 1. In SEM imaging, abrasive particle sizes were found to be less than 2 μm. The chemical composition of the abrasive particles used is given in Table 4.

In the study, a lubricant with a viscosity of 320 according to ISO 348 and a density of 895 kg/m3 at 15 °C was used. In the experiments, different environments were created by mixing the ore particle with the lubricant at 0.3 wt. % and 0.6 wt. %.

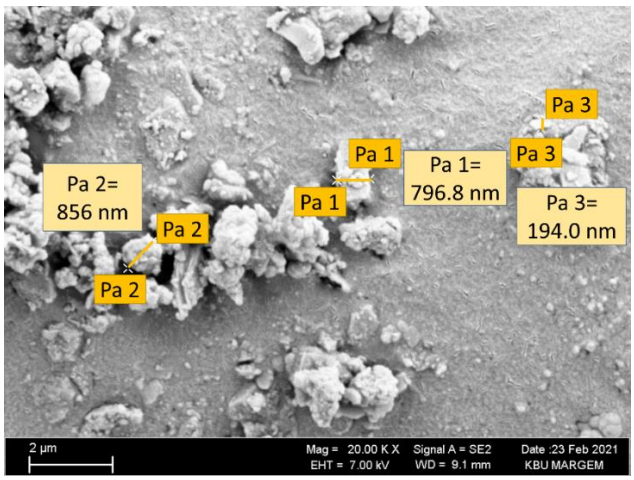

Figure 1. SEM image of abrasive ore particle and dimensional measurements

Table 4. Chemical composition of the abrasive particles

O	Fe	Si	Ca	Sb	Al	Others
63.49	19.25	5.99	4.72	2.69	1.71	2.15

2.3 Abrasive Test

Karabuk University Laboratories created the ball-on-flat wear test arrangement. The device can handle loads between 5 N and 65 N at 0 to 43.3 mm/s. During tests, a dynamometer measured force levels to calculate the friction coefficient. Figure 2 shows the device and technique schematics. Preliminary tests and literature reviews were used to determine the 20 - 40 - 60 N loads (Table 1), 17.3 – 30.3 – 43.3 mm/s sliding speeds, and sliding distance. Preliminary test traces were emphasized. After each experiment, MLs were measured with a 10-4 g balance. In the experiments, a 6 mm diameter ball made of 100Cr6 (AISI52100) material was selected and used as abrasive (Demirsoz et al., 2023).

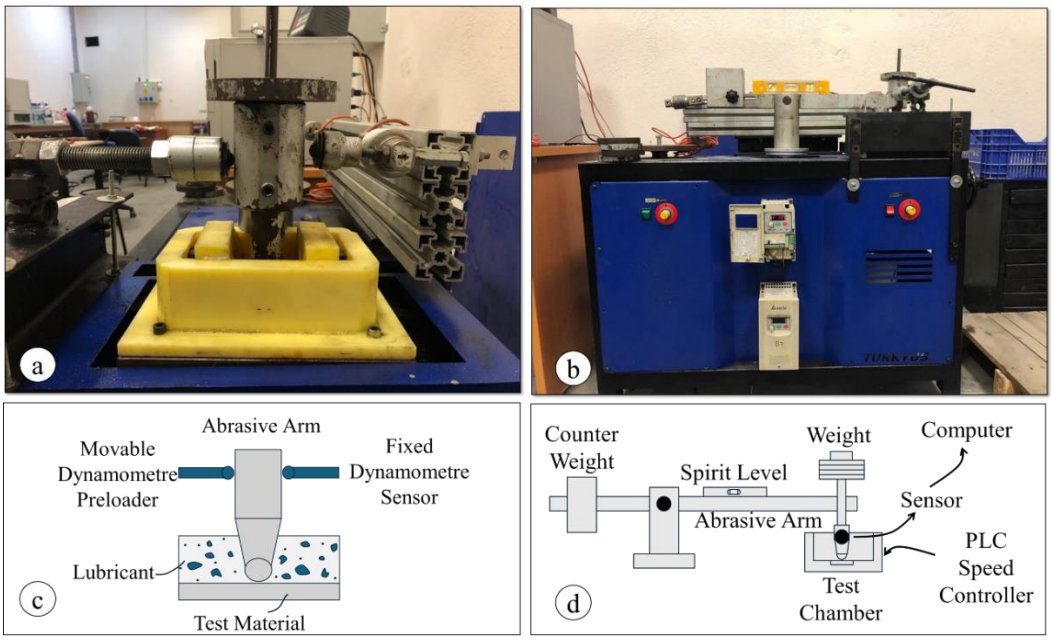

Figure 2. Photographs and schematic representations of the experimental device and the applied method a) abrasive arm and chamber, b) test setup, c) schematic representation of abrasive medium, d) schematic representation of test setup.

2.4 Experimental Design

TAGUCHI method is generally used in engineering experimental design. Performing full-variable experiments that will cover all parameters in multi-parameter test systems causes losses in terms of time and cost. For this reason, L9 (3x3) experimental design was created by Minitab program using TAGUCHI method (Rahiman et al., 2020; Sasidharan et al., 2018).

Load (N), rotational speed (rpm) and ore mass ratio in the lubricant were determined as independent variables for the test. Therefore, type of design is 3 level and number of factors is 3 (33) and the objective function were chosen as ,Smaller is Best,. Table 5 provides the TAGUCHI L9 orthogonal array control parameters.

Table 5. L9 Orthogonal array.

No	Load [N]	Sliding Speed [mm/s]	Concentration [wt. %]
1	20	17.3	0.0
2	20	30.3	0.3
3	20	43.3	0.6
4	40	17.3	0.3
5	40	30.3	0.6
6	40	43.3	0.0
7	60	17.3	0.6
8	60	30.3	0.0
9	60	43.3	0.3

3. RESULTS AND DISCUSSION

The ML values, CoF values, wear profiles and their signal to noise ratios obtained because of the work done with the C86200 material are given in the following section. The data obtained as a result of the experiments are given in Table 6.

Table 6. Ml, Cof and Td values obtained from the experiments.

No	L [N]	S [rpm]	C [%]	EML [mg]	ECoF	ETD [μm]
1	20	17.3	0.0	0.4 ±0.17	0.0888 ±0.0023	0.948 ±0.34
2	20	30.3	0.3	2.2 ±0.26	0.0933 ±0.0015	2.735 ±0.12
3	20	43.3	0.6	3.4 ±0.34	0.1299 ±0.0012	4.968 ±0.24
4	40	17.3	0.3	3.5 ±0.3	0.1222 ±0.0016	2.519 ±0.17
5	40	30.3	0.6	4.3 ±0.1	0.1396 ±0.0016	3.019 ±0.16
6	40	43.3	0.0	3 ±0.17	0.0804 ±0.0009	2.455 ±0.14
7	60	17.3	0.6	4.1 ±0.36	0.1447 ±0.0015	6.719 ±0.14
8	60	30.3	0.0	4.2 ±0.34	0.1005 ±0.0014	3.761 ±0.34
9	60	43.3	0.3	4.4 ±0.26	0.1181 ±0.0016	9.038 ±0.16

L: Load, S: Speed, C: Concentration, EML: Experimental Mass Loss, ECoF: Experimental Friction Coefficient, ETD: Experimental Trace Depth

In order to check the accuracy of the data, confirmation experiments were carried out with the optimum variables obtained from the Taguchi experimental design. Optimum variables for ML and TD outputs are 20 N at load, 50 rpm at slip velocity, and 0.3 wt. % at concentration. The ideal variables in the CoF outputs were found to be the load value of 40 N, the sliding speed value of 50 rpm, the concentration value, and the environment with only lubricant. The anticipated values and

the outcomes of the confirmation experiments are provided in Table 7. A confirmation experiment with a load value of 40 N, a sliding speed value of 50 rpm, and a lubricant-free environment free of abrasive particles is recommended by the Taguchi experimental design. These variable values presented for control purposes are one of the 9 experiments requested by Taguchi. For this reason, it was not necessary to conduct a control experiment for these values. When Table 7 is examined, the predicted result for the ML and CoF variables is 11.11% and 8.61% lower, respectively, then the value obtained as a result of the experiment. When the TD variable was examined, the predicted result value was 5.11% more than the experimental result value.

Table 7. Confirmation test result and predicted values.

No	L[N]	S[mn/s]	C %	EML [mg]	PML [mg]	ECoF	PCoF	ETD [μm]	PPD [μm]
6	40.0	43.3	0.0	3.0	3.2	0.0804	0.0873	2.455	2.503
15	20.0	43.3	0.3	2.7	2.4	0.0937	0.0986	4.851	5.099

L: Load, S: Speed, C: Concentration, EML: Experimental Mass Loss, PML: Predicted Mass Loss, ECoF: Experimental Friction Coefficient, PCoF: Predicted Friction Coefficient, ETD: Experimental Trace Depth PPD: Predicted Trace Depth.

The average values and probabilities of the ML, CoF and TD measurements obtained after the completion of the tests are given in Table 8. An analysis of variance was performed to determine what effect the load, sliding speed and environment parameters had on outputs such as ML, CoF and TD. The results from the wear test were used for statistical analysis. During this process, load (L), speed (S), concentration (C) were used as the variable source, while LxL, SxS and CxC were used as their relations. Significant and unimportant model terms were stated to be significant or insignificant according to the P index value being $P<0.05$ [(R. A. García-León et al., 2021b; Nas and Oztürk, 2018)].

Table 8. Anova values and contribution rates of load, speed and environment.

SoV	DF	ML	P Value	CoF	P Value	TD	P Value
Repetitions	3						
Test	27						
L	3	7.48167	0.05	0.000439	0.111	19.6819	0.013
S	3	1.30667	0.214	0.000124	0.367	6.5626	0.038
C	3	2.94	0.114	0.00348	0.019	9.4803	0.027
L x L	3	0.46722	0.395	0.000005	0.843	8.2459	0.03
S x S	3	0.37556	0.437	0.000017	0.698	3.2233	0.073
C x C	3	0.04957	0.76	0.000008	0.564	2.5137	0.09
Error	6	0.40444		0.000222		0.2625	
R^2		93.97%		94.84%		98.95%	
R^2(adj)		75.88%		79.37%		95.82%	
Contribution to wear test							
L		55.76%		10.20%		39.18%	
S		9.740%		2.88%		13.06%	
C		21.91%		80.91%		18.87%	
Error		6.02%		5.16%		1.05%	

SoV: Source of Variance, DF: Degrees of Freedom L: Load, S: Speed, C: Concentration, ML: Mass Loss, CoF: Friction Coefficient, TD: Trace Depth

Upon examining the R2(adj) values presented in Table 8, it is evident that the variables L, S, and C exert a significant influence on the ML, CoF, and TD outputs. When the P values obtained after the analysis are examined, it can be said that the P value for TD is significant. When the ML

and CoF columns are examined in the same table, P=0.05 is obtained only for the load variable in the ML column, and the result is significant (Cetin and Korkmaz, 2020) . The difficulty to entirely remove the oil that is still on the specimen surface and the embedding of the particles on the specimen surface are assumed to be the reasons why the P value is greater than 0.05.

It can be seen that some of the p values in the ML and CoF columns are greater than 0.05. The reasons for the high p value are thought to be very difficult to control events such as heating of the samples and abrasive, wear of the abrasive ball, and the inclusion of irregularly sized particles in the three-body wear mechanism.

3.1 Mass Loss (ML)

Specimen 9 yielded the largest ML when the MLs measured during the wear tests were analyzed (Table 6). The ML was determined to be 4.4 mg in this experiment with a 60 N load, a 43.3 mm/s sliding speed, and 0.3 weight percent ore. In specimen number 1, with a 20 N load, a 17.3 mm/s sliding speed, and a lubricating medium free of abrasive particles, the lowest ML was measured at 0.4 mg. It is evident that there are similarities between the actions of ML and TD. This condition may be related to increased load and speed as well as increased chip removal from the specimen surface by the abrasive particle plowing process, similar to what Mahajan and Peshwe found in their investigation. (Mahajan and Peshwe, 2018) .

When the ANOVA analysis were examined, it was concluded that the load parameter was effective on the ML at the rate of 55.76% and the lowest effect value on the ML was caused by the speed with a rate of 9.74%. Temperature change, vibration and material microstructure defects, etc., which are not included in the test variables and may affect ML. It can be said that the factors that are not included in the test variables constitute 6.02% error value. In the study, it was concluded that there is a strong interaction between ML and independent variables (R2(adj)=0.758). According to the results obtained, the ML changes significantly with the increase of the force. This situation can be associated with the increase in load and the removal of more material from the specimen surface by the plow mechanism of the abrasive particles.

S/N ratios were computed using the ‚Smaller is better, function in the study (Nas and Altan Özbek, 2020) . Figure 3a displays the plots that were obtained for experimental ML and S/N ratios. Additionally, Figure 3b displays the graph that illustrates the correlation between the experimental outcomes and the anticipated outcomes derived from the regression analysis of the ML values.

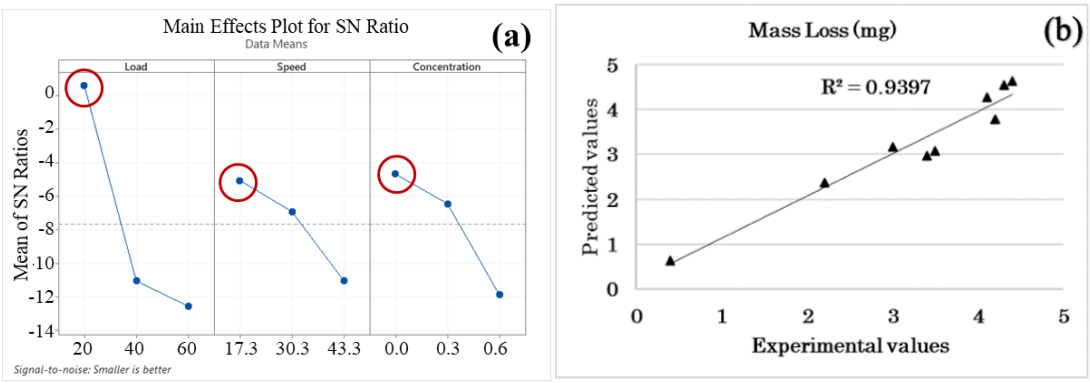

Figure 3. a) SN ratios for ML, b) the relationship between the experimental results and the predicted results of the ML values from the regression analysis

3.2 Friction Coefficient (CoF)

When the friction coefficients obtained after the wear tests were examined, the maximum CoF was obtained from the specimen number 7 (Table 6). In this experiment with a 60 N load, a 17.3 mm/s sliding speed, and 0.6 weight percent ore particles, the CoF was determined to be 0.1447. Specimen 6 had the lowest coefficient of friction, measuring 0.0804 at 43.3 mm/s sliding speed, 40 N load, and a lubricating liquid free of abrasive particles. Upon examination of the CoF data from the ANOVA analysis, it was determined that the concentration parameter had the highest effectiveness rate (80.91%) on CoF, while speed had the lowest effect value (2.88%) on CoF. Figure 4a displays the plots that were obtained for experimental CoF and S/N ratios. Figure 4b displays the graphs illustrating the correspondence between the experimental outcomes and the anticipated outcomes about the coefficient of determination (CoF) as derived from the regression analysis.

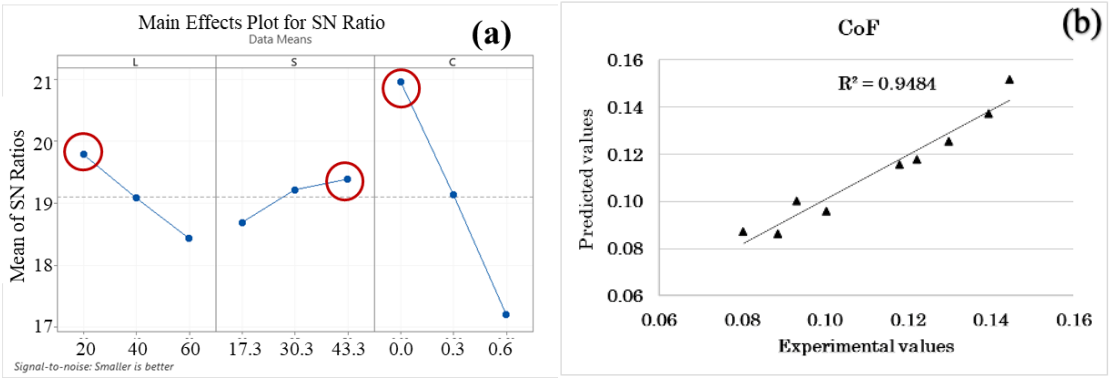

Figure 4. a) S/N ratios for CoF, b) the correlation between the outcomes of the experiment and the CoF values anticipated by the regression analysis

3.3 Trace Depth (TD)

When the TDs observed on the specimen surface after the abrasion tests were examined, the maximum TD was obtained from the specimen number 9 (Table 6). In this experiment, which had a 60 N load, a 43.3 mm/s sliding speed, and 0.3 weight percent ore particles, the minimum TD was measured at 9.038 µm. On specimen number 1, with a load of 20 N, a sliding speed of 117.3 mm/s, and a lubricating medium free of abrasive particles, the lowest TD was measured at 0.948 µm. The study's findings indicate that TD and independent variables have a significant interaction (R2(adj)=0.9582). Figure 5a displays the plots that were obtained for experimental TD and S/N ratios. Figure 5b displays the graphs that illustrate the correlation between the TD experimental findings and the anticipated outcomes derived from the regression analysis.

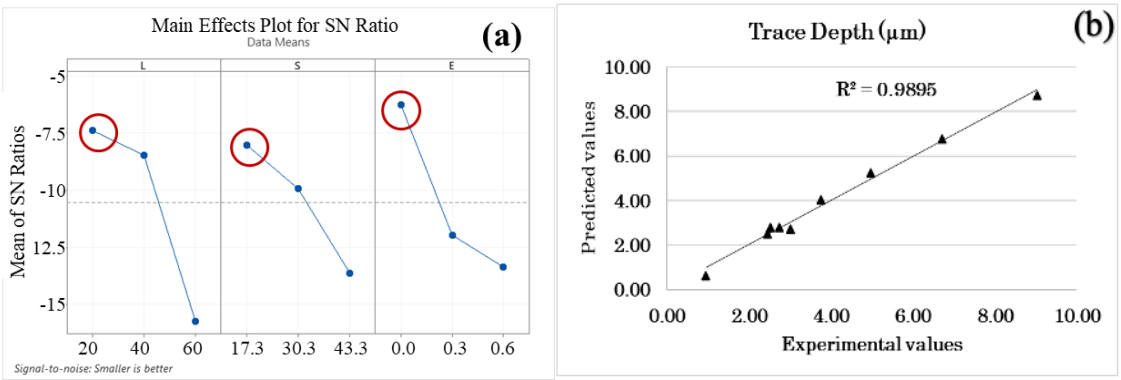

Figure 5. a) S/N ratios for TD, b) The relationship between experimental results and predicted results of the PD values from the regression analysis

3.4 Surface Observation

The wear profiles obtained by using a profilometer and the worn surface images obtained with the FESEM device are brought together in Figure 6, and the wear depth values are given in order from largest to smallest.

Examining the wear markings, it is clear that the specimens' wear marks—which were tested in a lubricating media containing 0.6% weight percent ore particles—are visible. Test specimens 9 with a 60 N load, 443.3 mm/s sliding speed, and 0.3% weight percentage of ore particles by weight were used to measure the maximum wear depth, which came out to be 9.038 µm. Conversely, test specimen No. 1 with a 20 N load, a 17.3 mm/s sliding speed, and an ore-free lubricating media yielded the lowest wear depth value, which was recorded at 0.948 µm.

Examining the wear surface profiles reveals that as the amount of particles increases, so do the wear surfaces' fluctuation and roughness. The wear profile fluctuates due to pegging and plowing mechanisms on the specimen surface, which can be explained by the rise in particle count in the environment (R. A. García-León et al., 2021b). Additionally, Bhoi et al. demonstrated that cutting lines on the degraded surface indicate ductile failure at high impact velocities (Bhoi et al., 2021). An example of a typical micro-ploughing process is seen in the worn debris, which suggests ductile failure.

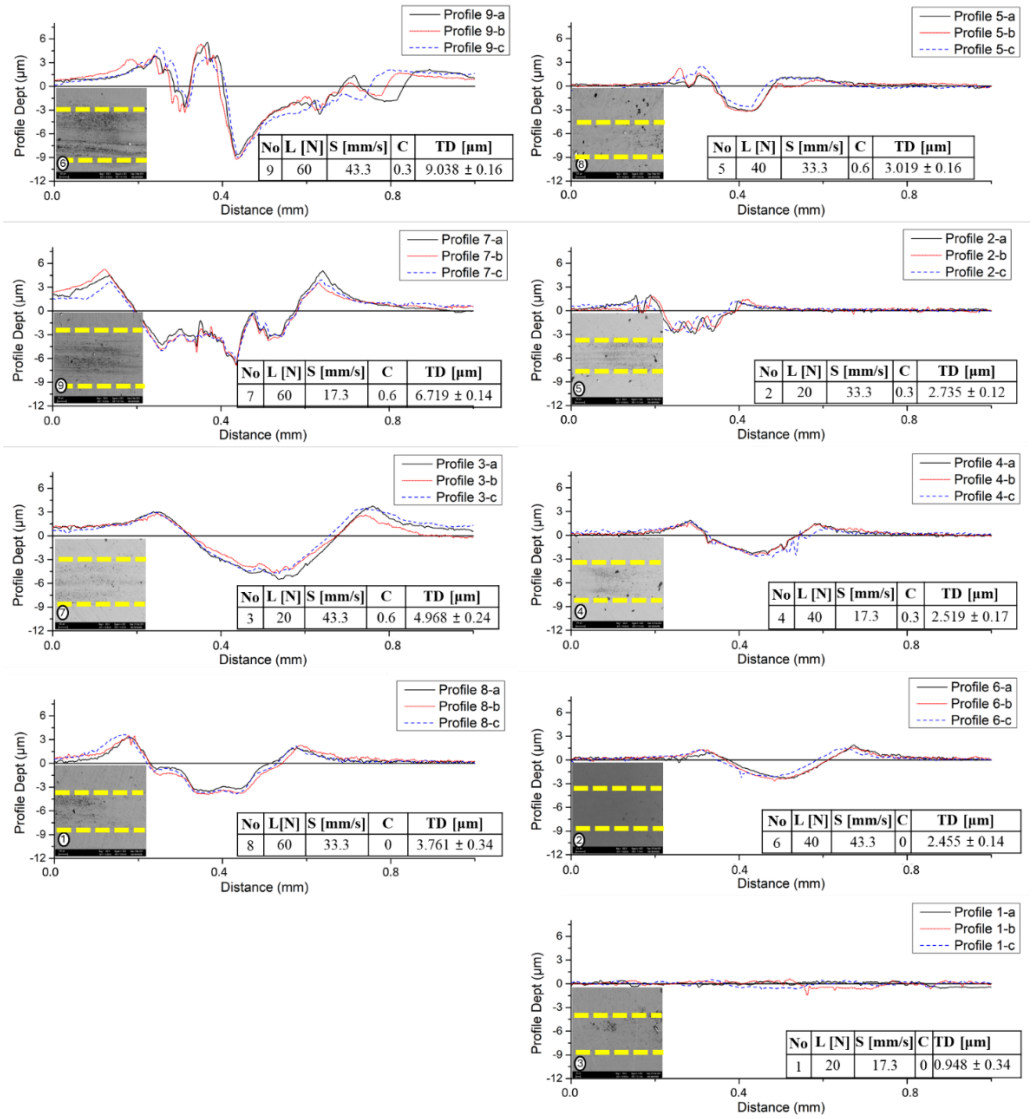

Figure 6. Wear trace profiles and worn surface images obtained from the SEM device

To observe the abrasive wear, 300X and 3kX magnified worn surface SEM images of specimen 7 are given in Figure 7. Upon analyzing the photos of the degraded surface, it was discovered that the ore particles were stuck to the surface. Abrasive ball chip particles of ore particles and bronze chip particles plow traces and related side extrude, and material agglomerations are observed. EDX analysis was performed to determine the components on the surface of the samples obtained, and EDX analyzes for some points and areas are given in Figure 8. In figure 8, EDX analysis was performed to determine what the bodies detected in the SEM images belonged to. In Figure 7, point P1 is thought to belong to the iron ore. Point P2 belongs to the sample. It is observed that in areas A1 and A2, iron ore, abrasive ball and elements belonging to the sample are mixed.

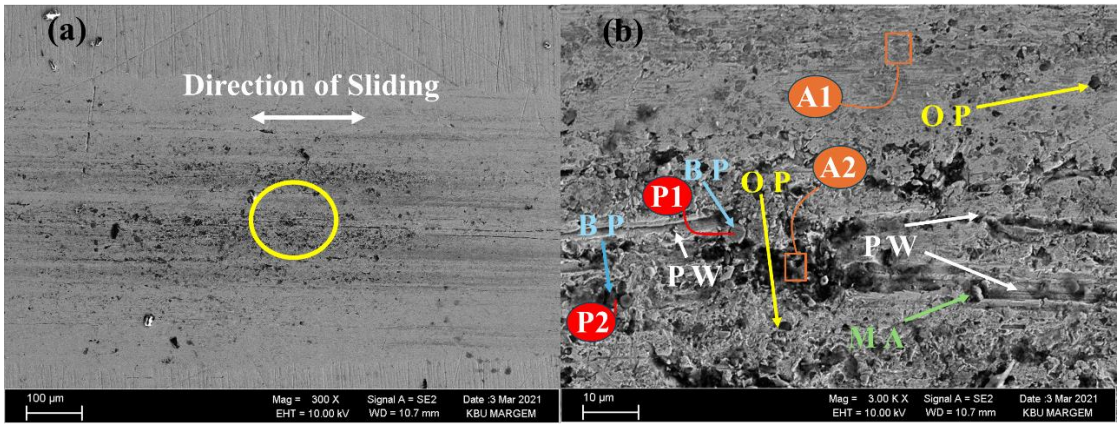

Figure 7. Wear mechanisms on the specimen surface a) 300X zoom, b) 3kX zoom. (OP: Ore Particle, PW: Plowing Wear, MA: Material Agglomeration, BP: Ball Particle)

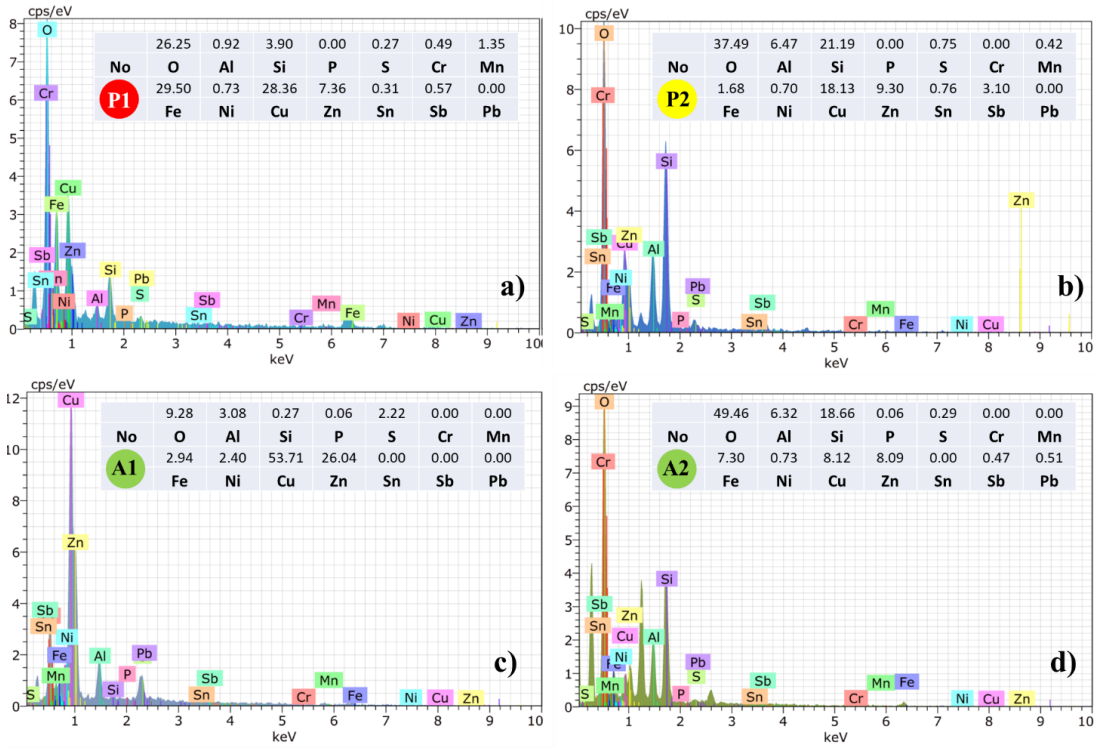

Figure 8. EDX analysis results of the points and areas on Figure 7 a) P1 point, b) P2 point, c) A1 area, d) A2 area.

4. CONCLUSION

This study investigated the effects of the three-body abrasive wear event on ML, coefficient of friction, and TD on the C86200 bronze material when micro-nano abrasive particles enter the lubricant using a ball-on-flat experiment design. The agreement between the predicted and experimental findings was assessed using the Response Surface Method. Furthermore, surface wear mechanisms were assessed based on EDX findings and SEM pictures.

The maximum ML was 4.4 mg (4.64 mg according to the predicted results) in the environment containing 60 N load, 43.3 mm/s sliding speed and 0.3 wt. % ore particles. Considering the predicted results, the highest wear value was obtained from the experiment with a 60 N load of 5.21 mg, a sliding speed of 43.3 mm/s and a medium containing 0.6 wt. % ore particles.

The highest CoF value was 0.1147 (0.1516 according to the predicted results) and 60 N load, 117.3 mm/s sliding speed and 0.6 wt. % ore particles were found in the environment. Considering the predicted results, the highest CoF value belongs to the experiment using the same parameters as the experimental parameters.

The highest TD value was 9.038 μm (8.721 μm according to the predicted results) with 60 N load, 43.3 mm/s sliding speed and 0.3 wt. % ore particles. Considering the predicted results, the highest value is 8.859 μm with 60 N load, 43.3 mm/s sliding speed and 0.6 % by weight of ore particles in the experiment.

5. ACKNOWLEDGEMENTS

The authors gratefully acknowledge Professor Hayrettin AHLATCI for his support in using the test device. The authors gratefully thank KARDOKMAK A.Ş. For their support in sample supply.

6. CONFLICT OF INTEREST

Author(s) approve that to the best of their knowledge, there is not any conflict of interest or common interest with an institution/organization or a person that may affect the review process of the paper.

7. AUTHOR CONTRIBUTION

Abdullah UĞUR contributed to the experiment design, data collection, and manuscript writing. Ahmet Emrah ERDOĞDU contributed to the execution of the experiments, the statistical analysis of the data, and manuscript editing. Recep DEMİRSÖZ contributed to the determination of the research concept, research management, interpretation of the findings, and manuscript editing.

8. REFERENCES

Akram, S, Babutskyi, A, Chrysanthou, A, Montalvão, D, Whiting, MJ, Pizurova, N: Improvement of the wear resistance of nickel-aluminium bronze and 2014-T6 aluminium alloy by application of alternating magnetic field treatment. Wear, 480–481: 2021.

Bailon-Poujol, I, Bailon, JP, L'Espérance, G: Ball-mill grinding kinetics of master alloys for steel powder metallurgy applications. Powder Technol, 210: 267–272, 2011.

Bharatish, A, Harish, V, Bathe, RN, Senthilselvan, J, Soundarapandian, S: Effect of scanning speed and tin content on the tribological behavior of femtosecond laser textured tin-bronze alloy. Opt Laser Technol, 108: 17–25, 2018.

Bhoi, S, Singh, RB, Harsha, AP, Manna, R: Effect of Grain Refinement on Tribological Study of Low Carbon Steel. Transactions of the Indian Institute of Metals, 74: 1489–1499, 2021.

Bozkurt, F, Çakir, Investigation of the Tribological and Mechanical Properties of Boron Steels in Terms of Potential Usage in Agricultural Applications. Politeknik Dergisi, 24: 431–438, 2021.

Cetin, M.H, Korkmaz, S: Investigation of the concentration rate and aggregation behaviour of nano-silver added colloidal suspensions on wear behaviour of metallic materials by using ANOVA method. Tribol Int, 147: 2020.

Demirsoz, R, Uğur, A, Erdoğdu, AE, Korkmaz, ME, Gupta, MK: Abrasive Wear Behavior of Nano-Sized Steel Scale on Soft CuZn35Ni2 Material. J Mater Eng Perform, 32: 8858–8869, 2023.

García-León, RA, Martínez-Trinidad, J, Campos-Silva, I, Figueroa-López, U, Guevara-Morales, A: Wear maps of borided AISI 316L steel under ball-on-flat dry sliding conditions. Mater Lett, 282: 17–18, 2021.

García-León, RA, Martínez-Trinidad, J, Zepeda-Bautista, R, Campos-Silva, I, Guevara-Morales, A, Martínez-Londoño, J, Barbosa-Saldaña, J: Dry sliding wear test on borided AISI 316L stainless steel under ball-on-flat configuration: A statistical analysis. Tribol Int, 157: 2021.

Gheisari, R, Polycarpou, AA: Three-body abrasive wear of hard coatings: Effects of hardness and roughness. Thin Solid Films, 666: 66–75, 2018.

Huang, L, Deng, X, Li, C, Jia, Y, Wang, Q, Wang, Z: Effect of TiC particles on three-body abrasive wear behaviour of low alloy abrasion-resistant steel. Wear, 434–435: 202971, 2019.

Kusumoto, K, Shimizu, K, Efremenko, VG, Hara, H, Shirai, M, ito, J, Hatate, M, gaqi, Y, Purba, RH: Three body type abrasive wear characteristics of multi-component white cast irons. Wear, 426–427: 122–127, 2019.

Lakshmikanthan, A, Bontha, S, Krishna, M, Koppad, PG, Ramprabhu, T: Microstructure, mechanical and wear properties of the A357 composites reinforced with dual sized SiC particles. J Alloys Compd, 786: 570–580, 2019.

Lan, P, Polycarpou, AA: High temperature and high pressure tribological experiments of advanced polymeric coatings in the presence of drilling mud for oil & gas applications. Tribol Int, 120: 218–225, 2018.

Lan, P, Polychronopoulou, K, Zhang, Y, Polycarpou, AA: Three-body abrasive wear by (silica) sand of advanced polymeric coatings for tilting pad bearings. Wear, 382–383: 40–50, 2017.

Liu, Q, Qi, F, Wang, Q, Ding, H, Chu, K, Liu, Y, Li, C: The influence of particles size and its distribution on the degree of stress concentration in particulate reinforced metal matrix composites. Materials Science and Engineering A, 731: 351–359, 2018.

Madhusudan, BM, Ghanaraja, S, Sudhakar, GN: Synthesis and development of size hybrid nano SiC-Al7075 composites by advanced stir casting. In: Materials Today: Proceedings. Elsevier Ltd, 2020, pp 3804–3809.

Mahajan, Y, Peshwe, DR: Effect of Temper Conditions on Abrasive Wear Behavior of AA7010 Alloy. Transactions of the Indian Institute of Metals, 71: 1025–1032, 2018.

Manoharan, S, Vijay, R, Lenin Singaravelu, D, Kchaou, M: Experimental Investigation on the Tribo-Thermal Properties of Brake Friction Materials Containing Various Forms of Graphite: A Comparative Study. Arab J Sci Eng, 44: 1459–1473, 2019.

Nas, E, Altan Özbek, N: Optimization of The Machining Parameters in Turning of Hardened Hot Work Tool Steel Using Cryogenically Treated Tools. Surface Review and Letters, 27: 1–14, 2020.

Nas, E, Oztürk, B: Optimization of surface roughness via the Taguchi method and investigation of energy consumption when milling spheroidal graphite cast iron materials. Materialpruefung/Materials Testing, 60: 519–525, 2018.

Purba, R. H., Shimizu, K., & Kusumoto, K: Three-Body Abrasive Wear-Resistance Characteristics of a 27Cr-Based 3V-3Mo-3W-3Co Multicomponent White Cast Iron with Different Ti Additions. Journal of Manufacturing and Materials Processing, 7(1), 21, 2023

Radhika, N, Sai Charan, K: Experimental Analysis on Three Body Abrasive Wear Behaviour of Stir Cast Al LM 25/TiC Metal Matrix Composite. Transactions of the Indian Institute of Metals, 70: 2233–2240, 2017.

Radhika, N: Mechanical Properties and Abrasive Wear Behaviour of Functionally Graded Al-Si12Cu/Al2O3 Metal Matrix Composite. Transactions of the Indian Institute of Metals, 70: 145–157, 2017.

Rahiman, AHS, Smart, DSR, Wilson, B, Ebrahim, I, Eldhose, B, Mathew, B, Murickan, RT: Dry sliding wear analysis OF Al5083/CNT/Ni/MoB hybrid composite using DOE Taguchi method. Wear, 460–461: 2020.

Sardar, S, Karmakar, SK, Das, D: Evaluation of Abrasive Wear Resistance of Al2O3/7075 Composite by Taguchi Experimental Design Technique. Transactions of the Indian Institute of Metals, 71: 1847–1858, 2018.

Sasidharan, S, Puthucode, R, Radhika, N, Shivashankar, A: Investigation of three body abrasive wear behaviour of centrifugally cast Cu-Sn/SiC functionally graded composite using Design of Experiment Approach. 2018.

Singh, RK, Telang, A, Das, S: The influence of abrasive size and applied load on abrasive wear of Al-Si–SiCp composite. Arab J Sci Eng, 47: 8617–8628, 2022.

Varol, T, Canakci, A, Ozsahin, S: Prediction of effect of reinforcement content, flake size and flake time on the density and hardness of flake AA2024-SiC nanocomposites using neural networks. J Alloys Compd, 739: 1005–1014, 2018.

Xin, W, Wang, YJ, Wei, SC, Liang, Y, Xia, XC, Chen, X, Wang, B, Xu, BS: Friction and wear behavior under oil lubrication conditions of amorphous-nanocrystalline composite coatings deposited via HVAS. Surf Coat Technol, 429: 2022.

Yin, YL, Yu, HL, Wang, HM, Song, ZY, Zhang, Z, Ji, XC, Cui, TH, Wei, M, Zhang, W: Friction and wear behaviors of steel/ bronze tribopairs lubricated by oil with serpentine natural mineral additive. Wear, 456–457: 2020.

Zhao, B, Zhang, Y, Fan, Y, Yu, X, Zhang, Z, Zhang, B: The three-body abrasive tribological characteristics of the Graphene/h-BN heterostructure film considering defects. Tribol Int, 171: 2022.